

Analysis of the Fabrication Process of Nb/Al-AlN_x/Nb Tunnel Junctions With Low $R_n A$ Values for SIS Mixers

N. N. Iosad, M. Kroug, T. Zijlstra, A. B. Ermakov, B. D. Jackson, M. Zuiddam, F. E. Meijer, and T. M. Klapwijk

Abstract—We characterize the fabrication process of superconductor-insulator-superconductor junctions (SIS) based on a Nb/Al-AlN_x/Nb tri-layer. Utilization of the AlN_x tunnel barrier, produced by Al nitridation in a nitrogen glow discharge, enables us to produce high quality SIS junctions with low $R_n A$ values (the product of junction resistance and area). Analyzing the correlation of junction resistance and plasma properties, it is concluded that the mechanism of tunnel barrier formation is based on nitrogen implantation into the Al layer with subsequent diffusion of nitrogen, stimulated by plasma heating. The latter process plays a dominant role since $R_n A$ values are well correlated with the power dissipated on the substrate surface. An SIS mixer using this technology and electron-beam lithography has been successfully fabricated.

Index Terms—Glow discharges, superconducting devices, tunneling.

I. INTRODUCTION

THE growth of AlN_x tunnel barriers by plasma nitridation was first reported by Lewicki and Mead [1]. Later Shiota *et al.* implemented these tunnel barriers in Nb/Al-AlN_x/Nb SIS junctions [2]. Furthermore, this process has been studied in greater detail and compared with the Nb/Al-AIO_x/Nb process by R. Dolata *et al.* [3]. However, this process failed to produce high quality SIS junctions with low $R_n A$ values [4]. This is due to the fact that a substrate located on a driven electrode is exposed to a very energetic and intense flux of ions during the Al nitridation [5]. Attaching the wafer to the electrode parallel to the driven electrode enables us to avoid the damage of the growing AlN layer by the energetic ions [5]–[7].

II. EXPERIMENTAL DETAILS

Tunnel junctions used for process characterization, are produced by a selective niobium anodization process on silicon wafers [8]. The size of all junctions is 10 μm². SIS junctions used for mixer production are made by the selective niobium etching process. The details of this process have been reported

Manuscript received August 6, 2002. This work was supported in part by FRBR project 00-02-16270, INTAS project 01-0367, and the ESA under Contract 11653/95.

N. N. Iosad, M. Kroug, T. Zijlstra, M. Zuiddam, F. E. Meijer, and T. M. Klapwijk are with the Department of Applied Physics (DIMES), Delft University of Technology, 2628 CJ Delft, The Netherlands (e-mail: iosad@tnw.tudelft.nl).

A. B. Ermakov is with Institute of Radioelectronics, the Russian Academy of Sciences, 103907, GSP-3 Moscow, Russia.

B. D. Jackson is with the National Institute for Space Research (SRON), 9700 AV, Groningen, The Netherlands.

Digital Object Identifier 10.1109/TASC.2003.813662

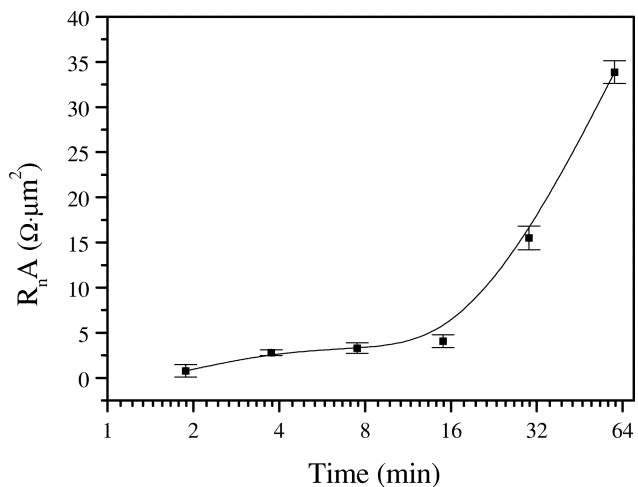


Fig. 1. Specific junction resistance versus nitridation time. The nitrogen pressure during Al layer nitridation is kept at 50 mTorr for all data points. Applied power during Al layer nitridation is kept at 30 W for all data points.

previously [9]. The layers of Nb and Al are sputtered by DC magnetrons at 8 mTorr Ar pressure. The deposition rates of Nb and Al are 100 nm/min and 20 nm/min, respectively. The thicknesses of the Nb bottom and top electrodes of SIS junctions are 300 nm and 50 nm respectively. The thickness of Al layer is 7 nm. The voltage-current characteristics (VCC) of the junctions are measured in liquid helium and characterized by a software program developed by Ermakov *et al.* [10]. The VCC are characterized on the basis of two key parameters: the specific junction resistance ($R_n A$), and the quality factor (R_{sg}/R_n , the ratio of the sub-gap and normal resistances). We use the $R_n A$ value rather than critical current density for junction characterization because this parameter is much easier and faster to measure. This fact is of great importance for us, since our research is based on the processing of a large number of junctions. Following the concept proposed by Bumble *et al.* the setup for Al nitridation has been implemented in a Nordiko-2000 sputtering system [6], [11]. The major difference between our system and the system developed by Bumble *et al.* is that the substrate is floating in our system. The technical details are published elsewhere [11].

A Langmuir probe, manufactured by Scientific Instruments, is employed for plasma characterization during the Al nitridation procedure. The probe is located 2 cm above the center of the substrate chuck. The flux of nitrogen ions bombarding the substrate during the nitridation procedure is characterized by two key parameters: the voltage drop across the substrate

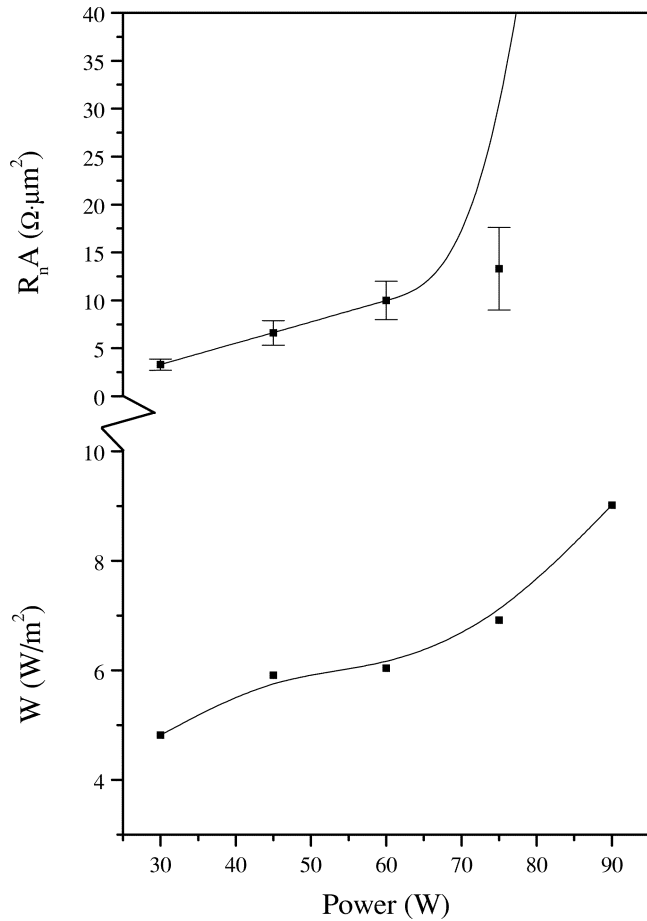


Fig. 2. Specific junction resistance and power density dissipated in the substrate sheath versus applied power. The nitrogen pressure is fixed at 50 mTorr for all data points.

sheath (V_{sh}), measured as a difference between the substrate and plasma potentials, and the ion current density injected into the sheath (J_i). The power density (W) dissipated on the substrate surface is estimated as a product of V_{sh} and J_i . Characterization of the plasma properties by the Langmuir probe revealed that V_{sh} values are very close to the plasma floating potential, indicating that the developed system produces the least possible plasma potential.

III. PARAMETRIC DRPENDENCE OF JUNCTION PROPERIETS

An investigation of the dependence of junction properties versus nitridation time was carried out under a nitrogen pressure fixed at 50 mTorr and an applied power fixed at 30 W. These settings result in the following nitrogen ion flux parameters: $J_I = 0.22 \text{ A/m}^2$ and $V_{sh} = 21 \text{ V}$. The discharge voltage is 240 V. Fig. 1 illustrates the dependence of $R_n A$ on nitridation time. Every data point represents an average of at least 20 junctions produced in one batch, with the error bars representing the standard deviation. Tunnel barrier formation in this experiment is a combination of two processes: (a) deposition of the sputtered AlN (the deposition rate is 6 \AA/h in this experiment). (b) nitridation of the Al layer. This process reaches saturation as seen from the plateau on the Fig. 1. Extra nitrogen implanted

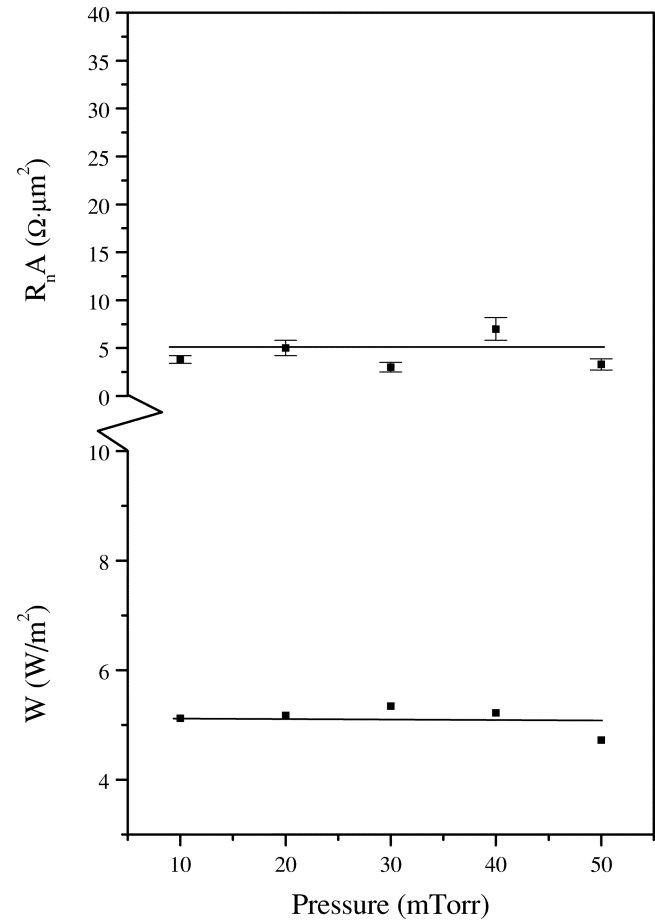


Fig. 3. Specific junction resistance and power dissipated in the substrate sheath versus nitridation pressure. Power is kept at the 30 W for all data points.

into the saturated AlN layer diffuses out. Similar behavior was observed by a number of authors [11]–[15].

Variation of the applied power, keeping the other parameters fixed (50 mTorr nitrogen pressure, 7 minutes nitridation time) results in an increase in $R_n A$ values (Fig. 2). The deposited thickness of AlN_x is negligible in this experiment, due to the short duration of the process. The voltage drop across the substrate sheath is almost constant ($V_{sh} = 18.5 \pm 1.5 \text{ V}$), while the dissipated power density increases rapidly with power (Fig. 2). The discharge voltage gradually increases with an increase in applied power (from 240 V to 496 V). It is interesting to mention that the spread in junction parameters over the wafer increases with $R_n A$ values in both this and in the previously mentioned experiment.

Variation of the nitrogen pressure, keeping the other parameters fixed (30 W applied power, 7 minutes nitridation time) does not result in significant changes in the $R_n A$ values (Fig. 3). The plasma parameters have very moderate dependence on nitrogen pressure: $J_i = 0.27 \pm 0.04 \text{ A/m}^2$, $V_{sh} = 18.8 \pm 2.2 \text{ V}$. The discharge voltage is almost independent of nitrogen pressure ($250 \pm 10 \text{ V}$), and the power density dissipated in substrate sheath is also almost constant (Fig. 3). The scale in this plot is made deliberately the same as in Fig. 2 to make the comparison with the previous experiment more vivid. This comparison clearly indicates that the process of Al nitridation is mainly governed by the power dissipated in the substrate sheath.

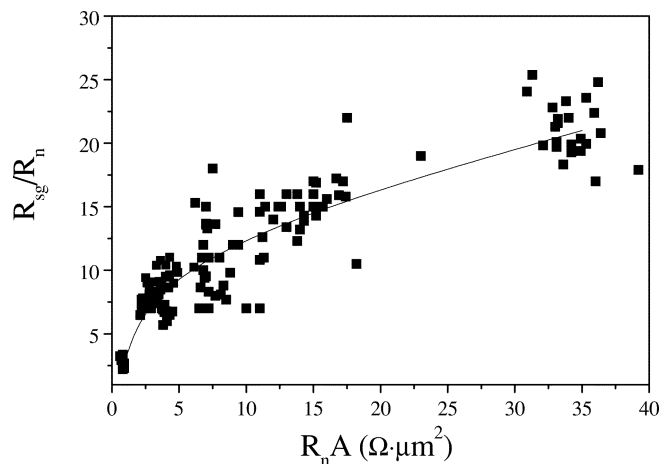


Fig. 4. Junction quality parameter R_{sg}/R_n versus specific junction resistance $R_n A$.

IV. ADDITIONAL RESULTS AND ANALYSIS

The diffusive mechanism also explains why AlN_x tunnel barriers are superior over AlO_x: the process of oxidation saturates at a much greater thickness (≈ 5 nm) than the process of nitridation (≈ 2 nm) [16]. The saturation of AlN_x growth at a thickness corresponding to low $R_n A$ values allows the sinks that are the source of pin-holes in the tunnel barriers to be saturated (Fig. 1). In contrast, the saturation of oxidation occurs at a tunnel barrier thickness that corresponds to ultra-high $R_n A$ values. In addition the utilization of an Al sub-layer (10 nm thick) in the middle of the bottom electrode of the SIS junction results in a substantial increase of $R_n A$ value without any degradation of junction quality, as in the case of Nb/Al-AIO_x/Nb SIS junctions [17]. Kohlstedt *et al.* explain an increase in AlO_x tunnel barrier resistance by smoothing of the Nb bottom electrode when an Al sub-layer is used [17]. This smoothing of the surface results in better wetting of the Nb surface by Al. This explanation is very doubtful because the surface of uncovered Nb islands is very difficult to oxidize or nitride up to the state of perfect tunnel barrier. We would like to propose another explanation. Both of these processes (oxidation and nitridation) have diffusive origin. The process of diffusion depends strongly on the density of sinks. Therefore it is reasonable to assume that the change in Nb roughness results in a different concentration of diffusion sinks in the Al layer. As a result, a substantial correction of the Al nitridation process is required when these junctions have to be integrated in various structures. In addition, despite different growth conditions there is a unique dependence of sub-gap leakage versus tunnel barrier resistance (Fig. 4). Every point on this plot corresponds to one junction. The degradation of the junction quality at low $R_n A$ values is due to heating and Multiple Andreev Reflections (MAR) [18]. Fig. 5 illustrates a characteristic MAR current step and back bending of the current rise at the gap voltage. In order to evaluate the limits of this technology, it is necessary to make junctions of sub-micron area. Dmitriev *et al.* have shown good quality junctions with $R_n A \approx 1 \Omega \cdot \mu\text{m}^2$ [19].

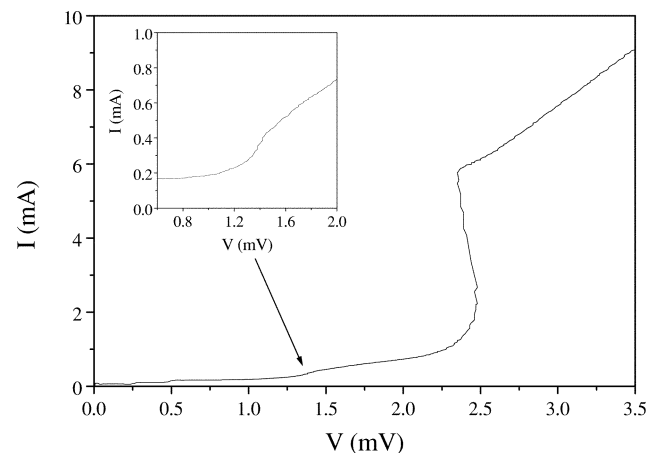


Fig. 5. VCC of SIS junction with $R_n A = 3.3 \Omega \cdot \mu\text{m}^2$. The MAR current step is illustrated on the insert. A magnetic field has been used to suppress the critical current.

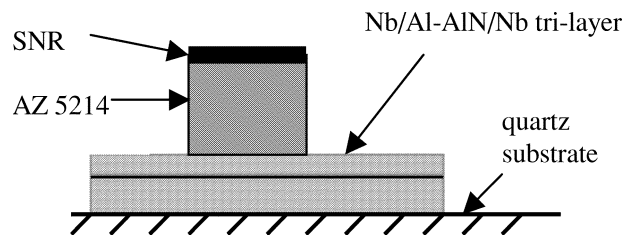


Fig. 6. Cross-sectional view of the junction definition process step.

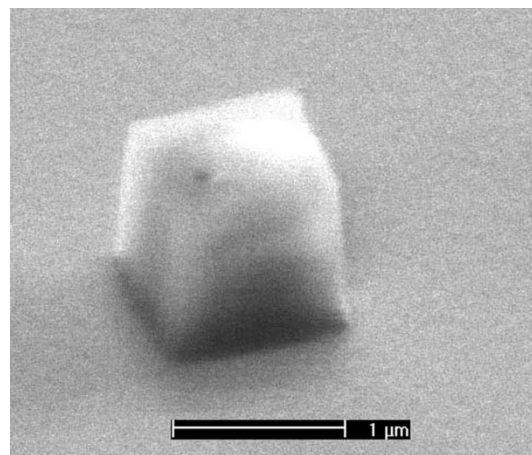


Fig. 7. SEM photograph of the photoresist pattern for junction definition.

V. MIXER FABRICATION

The major innovation compared to the previously described mixer fabrication process [9] is the use of an e-beam pattern generator for better junction definition. A double layer of resist (SNR e-beam resist and AZ 5214 conventional photoresist) is used in this case. The AZ 5214 is etched in oxygen plasma with a mask of e-beam resist by oxygen plasma (Fig. 6). The thick photoresist layer is needed to ensure the lift-off procedure after the deposition of the dielectric layer. The SEM picture illustrates perfect anisotropy of the etching process (Fig. 7). A typical VCC of a SIS mixer junction integrated into a Nb strip-line is illustrated in Fig. 8. The junction characteristics are much better

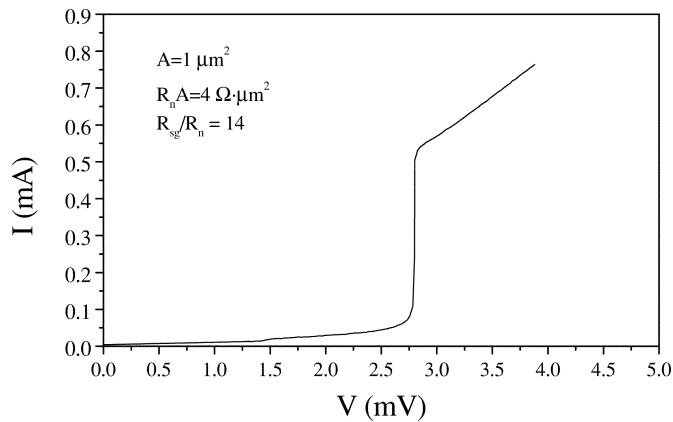


Fig. 8. VCC of SIS mixer junction integrated into Nb strip-line.

than that shown in Fig. 5 (with 10 times larger area) due to less heating effects. Preliminary results of AlN tunnel barriers in SIS mixers reveals good repeatability when the Nb bottom electrode roughness is taken into consideration.

VI. CONCLUSION

The fabrication process of SIS mixers equipped with Nb/Al-AlN/Nb tunnel junctions has been successfully implemented. Definition of the SIS junctions by means of e-beam lithography is successfully integrated into the fabrication process. This step enables better control over the junction size compared to optical lithography. The AlN tunnel barrier formation is carried out in a nitrogen RF glow-discharge with the substrate attached to the electrode parallel to the driven one. Analyzing the experimental data it is concluded that nitrogen diffusion into the Al layer facilitated by plasma heating is the main factor determining the tunnel barrier formation. The structure of the bottom Nb electrode of the SIS junction plays a significant role in the tunnel barrier formation, as in Nb/Al-AlO_x/Nb tunnel junctions. The reason for the increase of the spread of junction parameters over the wafer with an increase in $R_n A$ values is not yet understood. The typical energy of nitrogen ions bombarding the Al surface is in the order of 20 eV in our experiments. However the formation of the AlN layer takes place even if the energy of the bombarding nitrogen molecular ions is 1 eV. The latter fact indicates that the true potential of this process has not yet been reached [20]. AlN tunnel barriers produced with this technique are promising candidates for utilization in double tunnel barrier junctions for digital applications, since a very high transmissivity and quality of the tunnel barriers are also required for this application [21], [22].

REFERENCES

[1] G. Lewicki and C. A. Mead, "Experimental determination of E-k relationship in electron tunneling," *Phys.Rev. Lett.*, vol. 16, pp. 939-941, May 1966.

[2] T. Shiota, T. Imamura, and S. Hasuo, "Nb Josephson junction with an AlN_x barrier made by plasma nitridation," *Appl. Phys. Lett.*, vol. 61, pp. 1228-1230, September 1992.

[3] R. Dolata, M. Neuhaus, and W. Jutzi, "Tunnel barrier growth dynamics of Nb/AlO_x-Al/Nb and Nb/AlN_x-Al/Nb Josephson-junctions," *Physica C*, vol. 241, pp. 25-29, January 1995.

[4] A. W. Kleinsasser, W. H. Mallison, and R. E. Miller, "Nb/AlN/Nb Josephson-junctions with high critical-current density," *IEEE Trans. Appl. Supercond.*, vol. 5, pp. 2318-2321, June 1995.

[5] D. L. Smith, *Thin Film Deposition*. New York: McGraw-Hill, Inc, 1995, p. 406.

[6] B. Bumble, H. G. LeDuc, J. A. Stern, and K. G. Megerian, "Fabrication of Nb/AlN_x/NbTiN junctions for SIS mixer applications," *IEEE Trans. Appl. Supercond.*, vol. 11, pp. 76-79, March 2001.

[7] K. Kohler, J. W. Cobrun, D. E. Horne, E. Kay, and J. H. Keller, "Plasma potentials of 13.56-MHz rf argon glow discharges in a planar system," *J. Appl. Phys.*, vol. 57, pp. 59-66, January 1985.

[8] H. Kroger, L. N. Smith, and D. W. Jillie, "Selective niobium anodization process for fabricating Josephson tunnel junctions," *Appl. Phys. Lett.*, vol. 39, pp. 280-282, August 1981.

[9] N. N. Iosad, B. D. Jackson, T. M. Klapwijk, S. N. Polyakov, P. N. Dmitriev, and J. R. Gao, "Optimization of DC- and RF- sputtered NbTiN films for integration with Nb based SIS junctions," *IEEE Trans. Appl. Supercond.*, vol. 9, pp. 1716-1719, June 1999.

[10] A. B. Ermakov, S. V. Shitov, A. M. Baryshev, V. P. Koshelets, and W. Luinge, "A data acquisition system for test and control of superconducting integrated receivers," *IEEE Trans. Appl. Supercond.*, vol. 11, pp. 840-843, March 2001.

[11] N. N. Iosad, A. B. Ermakov, F. E. Meijer, B. D. Jackson, and T. M. Klapwijk, "Characterization of the fabrication process of Nb/Al-AlN_x/Nb tunnel junctions with low $R_n A$ values up to $1 \Omega \times \mu\text{m}^2$," *Supercond. Sci. Technol.*, vol. 15, pp. 945-951, June 2002.

[12] K. H. Park, B. C. Kim, and H. Kang, "Silicon nitride formation by low energy N⁺ and N₂⁺ ion beams," *J. Chem. Phys.*, vol. 97, pp. 2742-2749, August 1992.

[13] J. M. E. Harper, J. J. Cuomo, and H. T. G. Hentzell, "Synthesis of compound thin films by dual ion beam deposition. I. Experimental approach," *J. Appl. Phys.*, vol. 58, pp. 550-555, July 1985.

[14] R. P. Netterfield, K.-H. Muller, D. R. McKenzie, M. J. Goonan, and P. J. Martin, "Growth dynamics of aluminum nitride and aluminum oxide thin films synthesized by ion-assisted deposition," *J. Appl. Phys.*, vol. 63, pp. 760-769, February 1988.

[15] X. Wang, V. Charlamov, A. Koltisch, M. Posselt, Y. Trushin, and W. Moller, "Study of ion beam assisted deposition of Al/AlN multilayers by comparison of computer simulation and experiment," *J. Phys. D: Appl. Phys.*, vol. 31, pp. 2241-2244, August 1998.

[16] Z. Wang, H. Terai, A. Kawakami, and Y. Uzawa, "Interface and tunneling barrier heights of NbN/AlN/NbN tunnel junctions," *Appl. Phys. Lett.*, vol. 75, pp. 701-703, August 1999.

[17] H. Kohlstedt, F. Konig, P. Henne, N. Thyssen, and Caputo, "The role of surface roughness in the fabrication of stacked Nb/Al-AlO_x/Nb tunnel junctions," *J. Appl. Phys.*, vol. 80, pp. 5512-5514, November 1996.

[18] E. Scheer, P. Joyez, D. Esteve, C. Urbina, and M. H. Devoret, "Conduction channel transmissions of atomic-size aluminum contacts," *Phys. Rev. Lett.*, vol. 78, pp. 3535-3538, May 1997.

[19] P. N. Dmitriev, I. L. Lapitskaya, A. B. Ermakov, S. V. Shitov, G. V. Prokopenko, S. A. Kovtonyuk, and V. P. Koshelets, "High quality Nb-based integrated circuits for high frequency and digital applications," *IEEE Trans. Appl. Supercond.*, vol. 13, June 2003.

[20] S. Tzanev, A. Golichowski, W. Mix, and K. J. Snowdon, "Scattering of fast N₂, N₂⁺ and N₂²⁺ from Al(111) under glancing angles of incidence," *Surf. Sci.*, pp. 327-331, January 1995.

[21] M. I. Khabipov, D. V. Balashov, F. I. Buchholz, W. Kessel, and J. Niemeyer, "RSFQ circuitry realized in a SINIS technology process," *IEEE Trans. Appl. Supercond.*, vol. 9, pp. 4682-4687, December 1999.

[22] D. V. Balashov, Private Communication, October 2002.